

Ring formation of single-walled carbon nanotubes: Competition between conformation energy and entropy

Shengli Zhang,¹ Shumin Zhao,¹ Minggang Xia,¹ Erhu Zhang,¹ and Tao Xu²

¹*Department of Applied Physics, Xi'an Jiaotong University, Xi'an 710049, People's Republic of China*

²*Institute of Theoretical Physics, Chinese Academy of Science, P. O. Box 2375, Beijing 100080, People's Republic of China*

(Received 5 August 2002; revised 28 July 2003; published 22 December 2003)

We investigate ring formation of single-walled carbon nanotubes theoretically in this paper. The conformation energy of the nanotubes is identified as the curvature elastic energy of a curved graphite and the intertube van der Waals interaction. The entropy of ring nanotubes depends on the total number of carbon atoms. Assuming continuity, we find that the ring single-walled carbon nanotube is stable only when the radius of the tube is valued 6.958 Å. The ring diameter ranges from 200 to 700 nm.

DOI: 10.1103/PhysRevB.68.245419

PACS number(s): 61.48.+c, 68.03.Cd, 68.65.-k

I. INTRODUCTION

Carbon nanotube research¹⁻³ is now a very active field due to their unique properties and potential applications. Recent observations show that there are ring ropes of single-walled carbon nanotubes (SWNT's) (Refs. 4-9) which can be considered as quantum wires and which exhibit interesting transport properties.¹⁰⁻¹² These transport properties closely depend on the size of the ring SWNT making it important to find the optimal tube size and study the tube formation mechanisms in order to control their sizes during production fabrication.

Based on an SWNT coiling model, the thermodynamically stable ring diameter of ring SWNT's was calculated to have Young modulus $Y=1$ TPa and cohesive energy density $k=0.476$ eV. Assuming elasticity, 150 nm was found to be the smallest radius R of a defect-free carbon torus made from an SWNT whose radius r was around 1.4 nm.¹³ Models of carbon tori have been generated numerically where the kinks are synthesized at the atomic scale by inserting several pairs of pentagons and heptagons in a graphitic tubular network.^{10,14-21} Their geometry, electronic structure, and energy have been investigated by means of a tight-binding and semiempirical quantum chemical approach.²² The formation of ring multiwalled carbon nanotubes (MWNT's) has also been studied in terms of the continuum model.²³ However, the critical radius R_c for ring formation in Ref. 9 is smaller than that observed experimentally. Since the ring SWNT's appear as carbon nanotube ropes, the van der Waals interaction and entropy of SWNT's play important roles in their formation arrangement, which are not considered in Ref. 13. Because of the large number of carbon atoms, ring SWNT's on the sizes of experimental observation have not been studied numerically. Here, our investigation provides a theoretical study of the optimal ring and tube radius of ring SWNT's using the continuum model.

An SWNT, which often occurs in tightly packed triangular bundles,¹² can be thought of as a seamless cylinder wrapped in a graphitic sheet.²⁴ The van der Waals force plays an important role not only in the interaction of the nanotubes with the substrate but also in their mutual interaction. In this study we model a ring SWNT as a torus. The conformation

energy of the ring SWNT consists of the curvature elastic energy of the graphite layers E_b and the van der Waals interaction energy between graphite layers E_v . Therefore the free energy F of the ring SWNT is

$$F = E_b + E_v - TS, \quad (1)$$

where T is the generation temperature and S represents for the entropy of the tube.

In this paper, an approach to the free energies of ring SWNT's is given analytically to understand the formation mechanisms. We investigate the structure of ring SWNT's in terms of the continuum limit of the free energy. This paper is organized as follows: In Sec. II, the curvature elastic energy of a ring SWNT is studied in the continuum limit. In Sec. III, the van der Waals interaction energy within ring SWNT's is presented. In Sec. IV, the entropy of ring SWNT's is derived from their configuration. The optimal tube radius of the toroidal SWNT and ring diameter of ring SWNT's are determined in Sec. V. Finally, we give a conclusion in Sec. VI.

II. CURVATURE ELASTIC ENERGY OF TOROIDAL SWNT'S

The curvature elastic energy of a single layer curved graphite carbon tube has been proposed in terms of a two-dimensional lattice.²⁶ Assuming continuity the curvature elastic energy was expressed as follows:²⁷

$$E_b = \oint \left(\frac{1}{2} k_c (2H)^2 + k_g K \right) dA,$$

where H is the mean curvature, K is the Gaussian curvature of the tube surface, and dA stands for the differential area element of an SWNT surface. This curvature elastic energy has been applied in the study of fullerene clusters^{28,29} and in the study of SWNT helicity and MWNT formation.^{27,30-32} The bending rigidity k_c and saddle-splay modulus k_g have the dimension of energy. From the measured phonon spectrum of graphite, k_c has been found to be 1.2 eV.³³

According to differential geometry,²⁵ the Gaussian curvature contributes a topological invariant given by $\int K dA = \chi$,

where χ is the Euler characteristic for a surface. Applying this to the curvature elastic energy, the curvature elastic energy becomes

$$E_b = \frac{1}{2} k_c \oint (2H)^2 dA + k_g \chi. \quad (2)$$

As we have modeled ring SWNT's as tori, they can be parametrized in Cartesian coordinates,

$$\mathbf{Y} = \{\cos \theta (R - r \cos \phi), \sin \theta (R - r \cos \phi), r \sin \phi\}, \quad (3)$$

where R denotes the toroidal radius, r is the radius of the tube, and the parametric variables θ and ϕ range from 0 to 2π . Using Eq. (3), the first fundamental metric coefficients of the toroidal SWNT surface are given by²⁷

$$\begin{aligned} g_{11} &= (r \cos \phi - R)^2, \\ g_{12} &= g_{21} = 0, \\ g_{22} &= r^2, \end{aligned} \quad (4)$$

with

$$g = g_{11}g_{22} - g_{12}g_{21} = r^2(r \cos \phi - R)^2. \quad (5)$$

The second fundamental metric coefficients of the ring SWNT surface are determined by

$$\begin{aligned} L_{11} &= (r \cos \phi - R) \cos \phi, \\ L_{12} &= L_{21} = 0, \\ L_{22} &= r. \end{aligned} \quad (6)$$

In the derivation of Eqs. (6), we have used the unit normal vector of the toroidal SWNT surface $\mathbf{n} = \{\cos \phi \cos \theta, \cos \phi \sin \theta, \sin \phi\}$.

With Eqs. (4), (5), and (6) we derive that the mean curvature H and the differential area element dA :

$$H = \frac{1}{2} \left(\frac{\cos \phi}{r \cos \phi - R} + \frac{1}{r} \right), \quad (7)$$

and

$$dA = \sqrt{g} d\theta d\phi = r(R - r \cos \phi) d\theta d\phi. \quad (8)$$

Using the above expressions for H and dA , we obtain the curvature elastic energy for ring SWNT's,

$$E_b = \frac{2\pi^2 k_c R}{r \sqrt{1 - (r/R)^2}}. \quad (9)$$

In Eq. (9), we have applied the zero Euler characteristic for a torus ($\chi=0$).

III. VAN DER WAALS ENERGY OF RING SWNT'S

In this section, we calculate the van der Waals intertube adhesion energy E_v . This long-range dispersion interaction of a carbon-carbon pair is described at the atomic level by

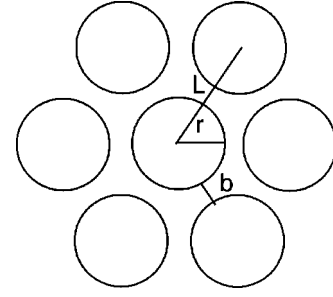


FIG. 1. Cross section of a toroidal SWNT rope is shown. The least possible distance between two neighboring tubes is $b = 3.4 \text{ \AA}$, r is the radius of a single tube, and $L = 2r + b$ is the distance between the centers of two adjacent tubes.

the Lennard-Jones potential, $u(d) = -A/d^6 + B/d^{12}$, where d is the carbon-carbon distance, $A = 15.16 \text{ eV \AA}^6$, and $B = 2.4 \times 10^4 \text{ eV \AA}^{12}$. A and B are characteristic of the attractive and repulsive interactions of the graphite^{34,35} respectively. The Lennard-Jones potential has been applied in the study of the radial deformation³⁶ and elastic properties of carbon nanotubes.³⁷

An approach to computing the total van der Waals energy is to employ a continuum model,^{38,39} so we will consider carbon nanotubes as continuous cylindrical surfaces. Since the occupied area per atom in an SWNT is $\sigma = (3\sqrt{3}/4)a^2$, where a stands for the stable distance between adjacent carbon atoms, one has the carbon atom density $n_\sigma = 4/(3\sqrt{3}a^2)$. In the continuum approximation, the van der Waals interaction energy between two identical and parallel tubes is

$$U = n_\sigma^2 \iint u(x) d\Sigma_1 d\Sigma_2, \quad (10)$$

where x is the distance between two surface elements $d\Sigma_1$ and $d\Sigma_2$ on two different tubes.

In Fig. 1 we show the cross section of a ring SWNT within its rope. Although there are only seven SWNT's in the figure, the number of ring SWNT's in the rope is not confined. And here we only plot the nearest neighbors of a ring SWNT, although this number, too, may vary. It can be seen that the tubes are arranged in a close-packed configuration, where r is the radius of a tube and $b = 3.4 \text{ \AA}$ is the least distance between two adjacent tubes. Because the main contribution of the van der Waals interaction energy between two tubes is in the vicinity of $b = 3.4 \text{ \AA}$, the interaction energy between two tubes whose separation distance is greater than this can be omitted. The formation energy of a ring with the toroidal rope is almost invariant as the number of tubes increases. It should also be noted that the number of nearest tubes to an outer tube is less than that of an inner tube generally. Because the total number of ring SWNT's is great,⁸ the number of the inner tubes is much large than that of the outtubes. The inner ring SWNT's play an major role in the formation of the toroidal ropes. We can neglect the contribution of the outer tubes and only deal with the inner tubes. From this simplified model, the van der Waals interaction energy between two carbon nanotubes can be calculated using Eq. (10).

The total van der Waals interaction energy between a toroidal SWNT and its neighboring tubes E_v is determined by summing U over all tube pairs. It can be written in the form

$$E_v = \frac{9\pi^2 n_\sigma^2 R}{2r^3} \left(-AI_A + \frac{21B}{32r^6} I_B \right) \quad (11)$$

with

$$I_A = \int_0^{2\pi} \int_0^{2\pi} \left[(\cos \theta_2 - \cos \theta_1)^2 + \left(\sin \theta_2 - \sin \theta_1 + \frac{L}{r} \right)^2 \right]^{-5/2} d\theta_1 d\theta_2, \quad (12)$$

$$I_B = \int_0^{2\pi} \int_0^{2\pi} \left[(\cos \theta_2 - \cos \theta_1)^2 + \left(\sin \theta_2 - \sin \theta_1 + \frac{L}{r} \right)^2 \right]^{-11/2} d\theta_1 d\theta_2, \quad (13)$$

where L is the distance between tube centers ($L = 2r + b$), and θ_1 and θ_2 range from 0 to 2π .

IV. ENTROPY OF RING SWNT

For a ring SWNT with ring radius R and tube radius r , its total area is $A = 4\pi^2 Rr$. Since the number of carbon atoms per unit area is $n_\sigma = 4/(3\sqrt{3}a^2)$, the total number of carbon atoms is given by

$$N = \frac{16\pi^2 Rr}{3\sqrt{3}a^2}, \quad (14)$$

where $a = 1.421 \text{ \AA}$. Because the radius of a tube in the ring must be less than or equal to the radius of the ring the SWNT must satisfy

$$r < r_{\max} = R_{\text{torus}} = \frac{a}{4\pi} \sqrt{3\sqrt{3}N}. \quad (15)$$

On the other hand, there is a lower limit for the tube radius of an SWNT. From the Gauss-Bonnet theorem,²⁵ we know that a torus can only be covered with hexagons. There must be at least three carbon hexagons along the tube circumference for its formation. Since the distance between two parallel bonds of a carbon hexagon is $\sqrt{3}a$, the minimum SWNT radius is

$$r_{\min} = \frac{3\sqrt{3}a}{2\pi}. \quad (16)$$

This is a (3,0) SWNT and has already been synthesized experimentally.⁴⁰

The radius of a (n, m) SWNT reads³

$$r = \frac{\sqrt{3}a}{2\pi} (n^2 + m^2 + nm)^{1/2}. \quad (17)$$

Using Eqs. (15) and (17), one has the maximum value of the integer n ,

$$n_{\max} = \left(\frac{1}{2} 3^{1/4} \sqrt{N} \right), \quad (18)$$

where $(\frac{1}{2} 3^{1/4} \sqrt{N})$ gives the greatest integer less than or equal to $\frac{1}{2} 3^{1/4} \sqrt{N}$.

In order to have a nonzero radius, $r > 0$, n and m are not allowed to be zero simultaneously. If $m = 0$ then we find the minimum of n from Eq. (16) as

$$n_{\min} = 3, \quad (19)$$

and vice versa for the case when $n = 0$.

In the case of a fixed total number of carbon atoms N , the maximum values of n and m are given by Eq. (18). One can label ring SWNT's according to the maximum value of their index n , which belongs to the set of all possible n , $n'_{\max} \in \{n_{\max}, n_{\max} - 1, \dots, 3\}$.

$$n'_{\max} = n_{\max}, n_{\max} - 1, \dots, 3. \quad (20)$$

For each fixed n'_{\max} , there are SWNT's with $(n'_{\max}, 0), (n'_{\max} - 1, 0), \dots, (3, 0)$. Therefore the total number of ring SWNT states for a fixed N is

$$\Omega = \frac{1}{2} (n_{\max} - 2)(n_{\max} + 3) = \frac{1}{2} (n_{\max}^2 + n_{\max} - 6). \quad (21)$$

From the definition of entropy, one has the structure entropy of ring SWNT's,

$$S_s = k_B \ln \Omega, \quad (22)$$

where k_B is the Boltzmann constant. Substituting Eq. (18) into Eq. (22), the structure entropy of a ring SWNT becomes

$$S = k_B \ln \left[\frac{1}{2} \left(\frac{\sqrt{3}}{2} N \right) + \frac{1}{2} \left(\frac{4\sqrt{3}}{\sqrt{2}} \sqrt{N} \right) - 6 \right]. \quad (23)$$

Under the continuum approximation, after substituting Eq. (14) into Eq. (23), we obtain

$$S = k_B \ln \left(4\pi^2 \frac{Rr}{a^2} + \frac{4\sqrt{3}}{\sqrt{2}} \pi \frac{\sqrt{Rr}}{a} - 6 \right). \quad (24)$$

On the other hand, mixing entropy is also a component in the free energy. Suppose there are M_{57} carbon pentagons in the network of carbon hexagons of the ring SWNT. We can infer from the Euler theorem in topology²⁵ that the number of heptagons is also M_{57} in the network of the ring SWNT in the case of the ring SWNT formed only by the pentagons, hexagons, and heptagons. Using the Bragy-Williams theory⁴⁰ we can derive the mixing entropy $S_m = M[-x \ln x - (1-x) \ln(1-x)]$, where M stands for the total number of carbon polygons (hexagons, pentagons, and heptagons) and $x = 2(M_{57}/M)$ is the ratio of the number of pentagons and heptagons to the polygons. Generally, the number of the pentagons and heptagons is far less than the number of the hexa-

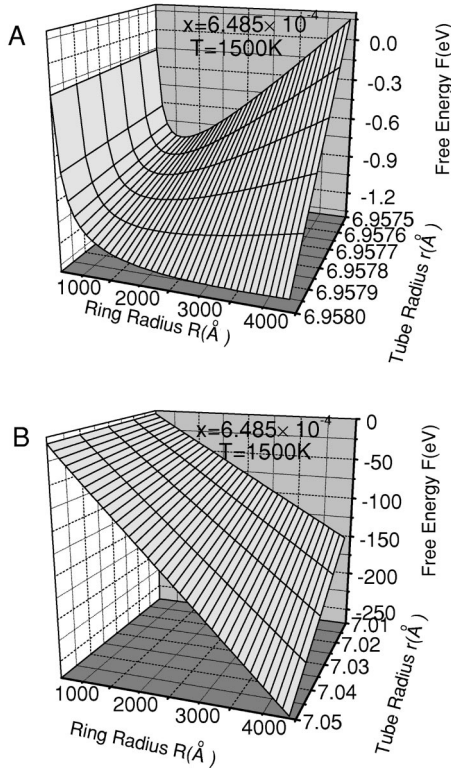


FIG. 2. The free energy is a function of the tube radius r and ring radius R for the fixed ratio x . (A) The free energy reaches its minimum values for $r < 7.01$ Å and $R < 3500$ Å. The synthesis temperature of ring SWNT's $T = 1500$ K. (B) The free energy decreases monotonically as R increases for $r > 7.01$ Å. There is not any minimum of the free energy in this region.

gons. Since each hexagon includes two carbon atoms, the number of the polygons M may be half of the number of carbon atoms, i.e., $M \approx N/2$. Then we have

$$S_m = \frac{8\pi^2 R r}{3\sqrt{3}a^2} k_B \ln[-x \ln x - (1-x) \ln(1-x)] \quad (25)$$

in which we have used Eq. (14).

The total entropy of ring SWNT's is the summation of the structure entropy S_s and the mixing entropy S_m .

V. OPTIMAL TUBE RADIUS AND RING DIAMETER OF TOROIDAL SWNT

Using the curvature elastic energy (9), van der Waals energy (11), entropy (24), and Eq. (25), the free energy of the ring SWNT can be subsequently expressed as

$$F = E_b + E_v - T(S_s + S_m) = \frac{2\pi^2 k_c R}{r\sqrt{1-(r/R)^2}} - \frac{9\pi^2 n_\sigma^2 R}{2r^3} \left(-AI_A + \frac{21B}{32r^6} I_B \right) - k_B T \ln \left(4\pi^2 \frac{Rr}{a^2} + \frac{\sqrt[4]{3}}{\sqrt{2}} \pi \frac{\sqrt{Rr}}{a} - 6 \right) - k_B T \frac{8\pi^2 R r}{3\sqrt{3}a^2} k_B \ln[-x \ln x - (1-x) \ln(1-x)]. \quad (26)$$

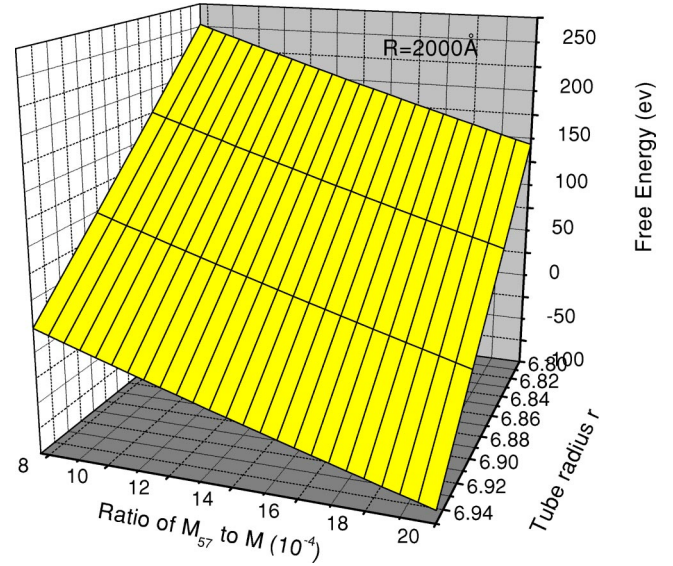


FIG. 3. The free energy depends on the tube radius r and the ratio x for the fixed ring radius R . It decreases monotonically as r and x increase. The synthesis temperature of ring SWNT's $T = 1500$ K.

In Eq. (26) I_A and I_B are two functions of the tube radius defined by Eqs. (16) and (17), respectively, $n_\sigma = 4/(3\sqrt{3}a^2)$, and T stands for the synthesis temperature of ring SWNT's.

From Eq. (26) we can study the optimal structure of ring SWNT's which is determined by the equilibrium condition $\delta F = 0$. Note that carbon nanotubes grow from an initial tubular nucleus with the fixed radius.⁴¹ The equilibrium shape of the SWNT is determined by minimizing the free energy with respect to the torus radius, and the number ratio of pentagons to total polygons. In other words, the stable formation of a ring SWNT is found by the minimum of its free

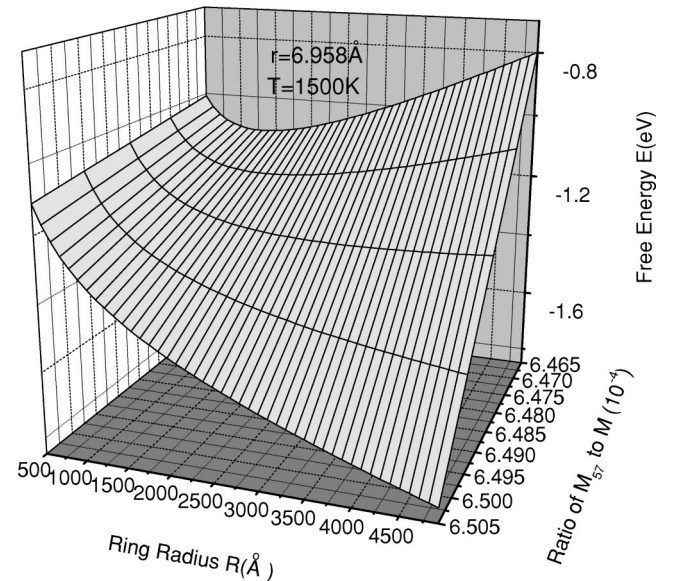


FIG. 4. The free energy varies with the ratio x and the ring radius R . The free energy is minimum only when $x < 6.495 \times 10^{-4}$. The synthesis temperature of ring SWNT's $T = 1500$ K.

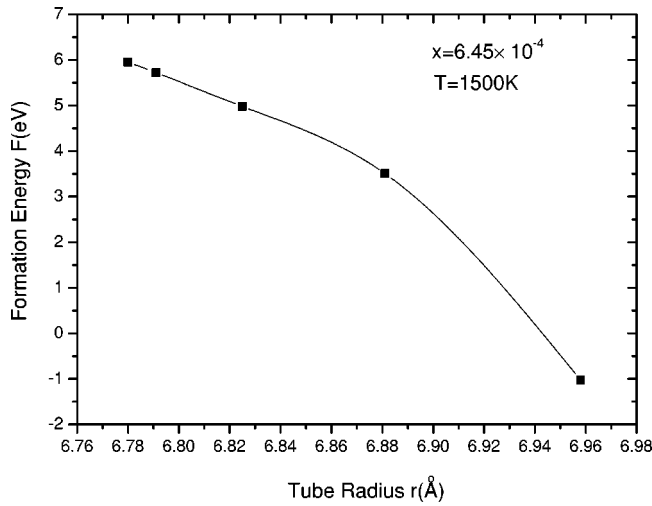


FIG. 5. The formation energy versus the tube radius r is plotted for the case of $x = 6.45 \times 10^{-4}$. It decreases with r when $r < 7.01$ Å. The synthesis temperature of ring SWNT's $T = 1500$ K.

energy with respect to the torus radius R , and the ratio x . We call the minimum of the free energy the formation energy. The free energy is a function of the tube radius r , the ring radius R , and the ratio x . Simulating the free energy numerically, we plot it in Figs. 2–4. The relationships between the formation energy and the tubal radius, ring radius, and the ratio of the toroidal SWNT are presented in Figs. 5–7, respectively. This formation energy forms the basis of our investigation of the optimal tubal radius and ring radius of the ring SWNT's.

Through numerical calculation, as Fig. 2, we find that the free energy decreases with increasing ring radius R when $r > 7.01$ Å. There is no minimum for arbitrary x if $r > 7.01$ Å. Figure 5 shows there are no values for the formation energy when $r > 7.01$ Å which means there is also no stable formation of ring SWNT's in this case. Thus investigations of the optimal structure of ring SWNT's must be

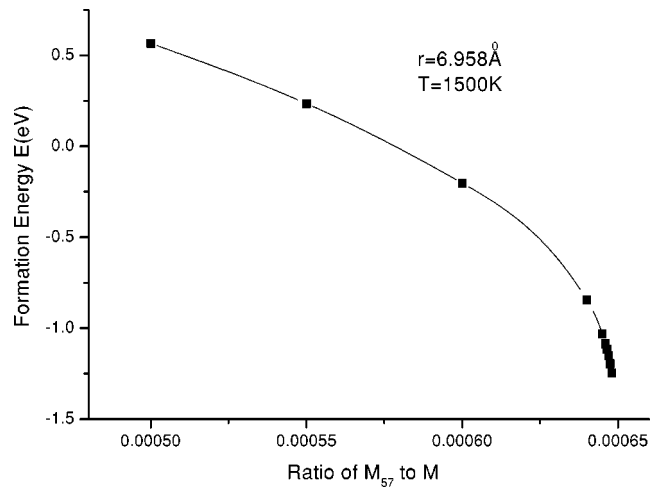


FIG. 6. For the fixed radius $r = 6.958$ Å, i.e., (14,6) SWNT, the formation energy varies with the ratio x . When $x > 6.495 \times 10^{-4}$, there is no value. It decreases as x increases when $x < 6.495 \times 10^{-4}$. The synthesis temperature of ring SWNT's $T = 1500$ K.

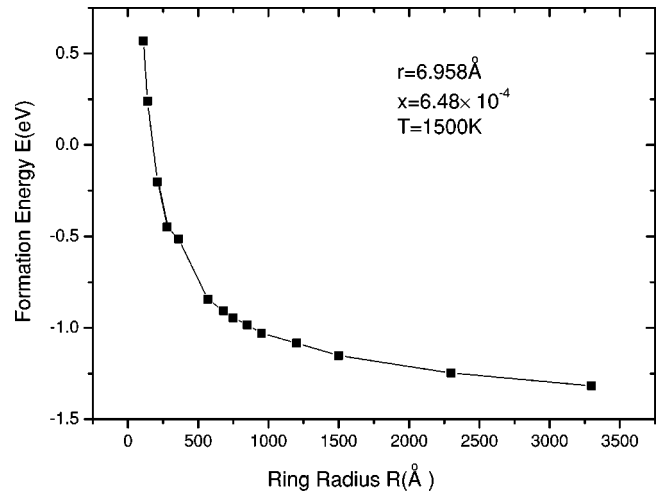


FIG. 7. The formation energy decreases monotonically as ring radius R increases for the fixed tube radius r and ratio x .

carried out in the region of $r \leq 7.01$ Å. For fixed ring radius, the free energy decreases monotonically as the tube radius r and the ratio x increase (see Fig. 3). Calculating tube radius by means of $r = (\sqrt{3}a/2\pi)\sqrt{n^2 + m^2 + mn}$,² where m and n are two integers characterizing the structure of an SWNT, one finds that a (14,6) carbon nanotube is optimum. We conclude that ring SWNT's are most stable for $r = 6.958$ Å, i.e., (14,6) SWNT.

Similarly, one sees from Fig. 4 that the free energy decreases with ring radius R when $x > 6.495 \times 10^{-4}$. There is also no minimum energy regardless of r in the case of $x > 6.495 \times 10^{-4}$. From Fig. 6 we find there are no values for the formation energy when $x > 6.495 \times 10^{-4}$, which means there is no stable formation of ring SWNT's in this case, and so we must deal with carbon nanotubes in the region $x < 6.495 \times 10^{-4}$. As in Fig. 3, the free energy decreases with the ratio x . The formation energy also decreases with x (see

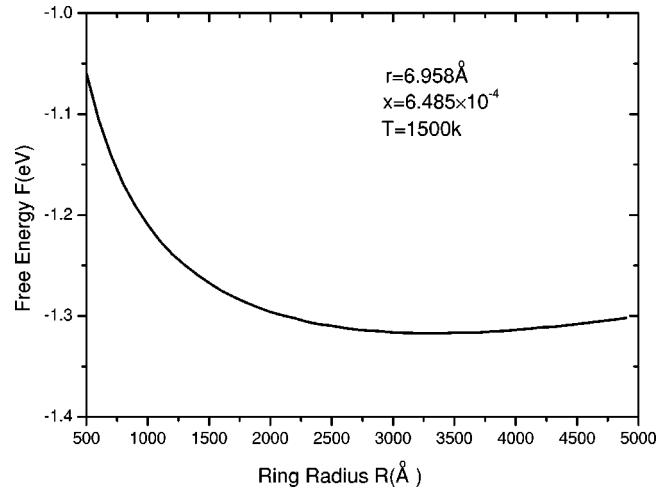


FIG. 8. The free energy is a function of the ring R when $r = 6.958$ Å and $x = 6.485 \times 10^{-4}$. Its minimum is $F_{\min} = -1.317$ eV, which corresponds to $R = 3500$ Å. The synthesis temperature of ring SWNT's $T = 1500$ K.

Fig. 6). Furthermore, the variation step of the ratio x is $\Delta x = 2/M = 1/N$. Using Eq. (14) and data in Ref. 4, one can obtain $\Delta x \sim 10^{-6}$. So we can reasonably take $x = 6.485 \times 10^{-4}$ as the optimal value of the ratio $2M_{57}/M$ in our investigation.

When $r = 6.958 \text{ \AA}$ and $x = 6.485 \times 10^{-4}$, the free energy versus the ring radius R is plotted as Fig. 8. It is clear that $R = 3500 \text{ \AA}$ is the optimum ring radius of the ring SWNT, which corresponds to the minimum of the free energy. We note that the entropy makes the free energy increasing for $r < 7.01 \text{ \AA}$ and $R > 3500 \text{ \AA}$ although the curvature elastic energy is reduced in this case.

From Fig. 8, we find that the minimum formation energy $F_{\min} = -1.317 \text{ eV}$ occurs when $R = 3500 \text{ \AA}$. On the other hand, due to thermal fluctuations the formation energy of the ring SWNT can range from F_{\min} to $F_{\min} + k_B T$, where k_B is the Boltzmann constant and T stands for the absolute temperature. For the growth temperature $T = 1500 \text{ K}$,⁴ at which the two ends of the SWNT's weld together, we have $k_B T \approx 0.129 \text{ eV}$. One can calculate $100 \leq R \leq 350 \text{ nm}$ when the free energy ranges from $F_{\min} = -1.317 \text{ eV}$ to $F_{\min} + k_B T = -1.188 \text{ eV}$. Therefore the optimal ring diameter is $200 \leq 2R \leq 700 \text{ nm}$.

VI. CONCLUSION

In conclusion, we have explained experimental observations of SWNT's in terms of free energy, which consists of curvature elastic energy, van der Waals interaction, and the entropy of ring nanotubes. A balance between conformation energy (curvature elastic energy and van der Waals energy) and entropy generates ring SWNT's optimal structures. The fluctuation of ring SWNT's formation energy determines the size distribution of the ring SWNT's. We derive the optimal tube radius to be $r \approx 6.958 \text{ \AA}$ for ring SWNT's. The optimal ring diameter is shown to range from 200 to 700 nm, which is also in the region of experimental observations.⁴

ACKNOWLEDGMENTS

This work was supported by the NSF of China (Grant No. 19875053), the Excellent Young Teachers Program of MOE, P.R. China, and University Key Teacher Foundations of MOE, P.R. China.

- ¹S. Iijima, *Nature (London)* **354**, 36 (1991).
- ²R. Saito, G. Dresselhaus, and M. S. Dresselhaus, *Physical Properties of Carbon Nanotubes* (Imperial College Press, London, 1998).
- ³M. S. Dresselhaus, G. Dresselhaus, and Ph. Abouris, *Carbon Nanotubes Synthesis, Structure, Properties, and Applications* (Springer-Verlag, Berlin, 2001).
- ⁴J. Liu, H. Dai, J.H. Hafner, D.T. Colbert, R.E. Smalley, S.J. Tans, and C. Dekker, *Nature (London)* **385**, 780 (1997).
- ⁵J. Liu, A.G. Rinzier, H. Dai, J.H. Hafner *et al.*, *Science* **280**, 1253 (1998).
- ⁶M. Ahlskog, E. Seynaeve, R.J.M. Vullers, C. Van Haesendonck, A. Fonseca, K. Hernadi, J.B. Nagy, *Chem. Phys. Lett.* **300**, 202 (1999).
- ⁷M. Sano, A. Kamino, and J.D. Shinkai, *Science* **293**, 1299 (2001).
- ⁸R. Martel, H.R. Shea, and P. Avouris, *Nature (London)* **398**, 299 (1999).
- ⁹R. Martel, H.R. Shea, and P. Avouris, *J. Phys. Chem. B* **101**, 7551 (1999).
- ¹⁰R.C. Haddon, *Nature (London)* **388**, 31 (1997).
- ¹¹J. Rollbuintsov, *Physica B* **280**, 483 (1996).
- ¹²A. Thess, R. Lee, P. Nikolaev, H. Dai *et al.*, *Science* **273**, 483 (1996).
- ¹³V. Meunier, Ph. Lambin, and A.A. Lucas, *Phys. Rev. B* **57**, 14 886 (1998).
- ¹⁴B.I. Dunlap, *Phys. Rev. B* **46**, 1933 (1992).
- ¹⁵S. Itoh, S. Ihara, and J. Kitakami, *Phys. Rev. B* **47**, 1703 (1993).
- ¹⁶R. Setton and N. Setton, *Carbon* **35**, 497 (1997).
- ¹⁷J.K. Johnson, B.N. Davidson, M.R. Pederson, and J.Q. Broughton, *Phys. Rev. B* **50**, 17 575 (1994).
- ¹⁸J.C. Greer, S. Itoh, and S. Ihara, *Chem. Phys. Lett.* **222**, 621 (1994).
- ¹⁹B. Birstnik and D. Lukman, *Chem. Phys. Lett.* **228**, 31 (1994).
- ²⁰S. Ihara, S. Itoh, and J. Kitakami, *Phys. Rev. B* **47**, 12 908 (1993).
- ²¹S. Itoh and S. Ihara, *Phys. Rev. B* **48**, 8323 (1993).
- ²²D.H. Oh, J.M. Park, and K.S. Kim, *Phys. Rev. B* **62**, 1600 (2000).
- ²³S.-L. Zhang, *Phys. Rev. B* **65**, 235411 (2002).
- ²⁴S. Iijima *et al.*, *Nature (London)* **356**, 776 (1992).
- ²⁵M.P. do Carmo, *Differential Geometry of Curves and Surfaces* (Prentice-Hall, Englewood Cliffs, NJ, 1976).
- ²⁶T. Lenosky, X. Gonze, M. Teter, and V. Elser, *Nature (London)* **355**, 333 (1992).
- ²⁷O.Y. Zhong-can, Z.B. Su, and C.L. Wang, *Phys. Rev. Lett.* **78**, 4055 (1997).
- ²⁸V.V. Rotkin and R.A. Sunis, in *Fullerencess: Recent Advances in the Chemistry and Physics of Fullerenes and Related Materials*, edited by R.S. Ruoff and K.M. Kadish (Electrochemical Society, Pennington, NJ, 1995), pp. 1263–1270.
- ²⁹S.V. Rotkin and R.A. Suries, in *Computational and Mathematical Models of Microstructural Evaluation*, edited by J. W. Bullard, L.-Q. Chen, R. K. Kalia, and A. M. Stoneham (CRS, Warrendale, PA, 1998), pp. 175–180.
- ³⁰S.-L. Zhang, S.-M. Zhao, J.-Y. Lu, and M.-G. Xia, *Phys. Rev. B* **61**, 12 693 (2000).
- ³¹S.-L. Zhang, *Phys. Lett. A* **785**, 207 (2001).
- ³²M.T. Yu, T. Kowalewski, and R.S. Ruoff, *Phys. Rev. Lett.* **86**, 87 (2001).
- ³³L. Henrard, E. Hernandez, P. Bernier, and A. Rubio, *Phys. Rev. B* **60**, R8521 (1999).
- ³⁴L.A. Girifalco and R.A. Lad, *J. Chem. Phys.* **25**, 693 (1956).
- ³⁵R.S. Ruoff and J. Tersoff, *Nature (London)* **364**, 514 (1993).
- ³⁶J.P. Lu, *Phys. Rev. Lett.* **79**, 1297 (1999).
- ³⁷J. Tersoff and R.S. Ruoff, *Phys. Rev. Lett.* **73**, 676 (1994).

³⁸L.A. Girifalco, M. Hodak, and R.S. Lee, Phys. Rev. B **62**, 13 104 (2000).

³⁹N. Wang, Z.K. Tang, G.D. Li, and J.S. Chen, Nature (London) **408**, 50 (2000).

⁴⁰P. M. Chaikin and T. C. Lubensky, *Principles of Condensed Mat-*

ter Physics (Cambridge University Press, Cambridge, England, 1995).

⁴¹P. Zhang and V.H. Crespi, Phys. Rev. Lett. **83**, 1791 (1999), and references therein.